# Delft University of Technology

## Tropical rainfall monitoring with commercial microwave links in Sri Lanka

Overeem, Aart; Leijnse, Hidde; van Leth, Thomas C.; Bogerd, Linda; Priebe, Jan; Tricarico, Daniele; Droste, Arjan; Uijlenhoet, Remko

**LETTER • OPEN ACCESS**

# Tropical rainfall monitoring with commercial microwave links in Sri Lanka

View the article online for updates and enhancements.

# ENVIRONMENTAL RESEARCH
## LETTERS

**LETTER**

# Tropical rainfall monitoring with commercial microwave links in Sri Lanka

Aart Overeem[1,2,*] ![ID], Hidde Leijnse[1,2] ![ID], Thomas C van Leth[2] ![ID], Linda Bogerd[1,2] ![ID], Jan Priebe[3], Daniele Tricarico[3], Arjan Droste[2] ![ID] and Remko Uijlenhoet[2,4] ![ID]

1  R&D Observations and Data Technology, Royal Netherlands Meteorological Institute (KNMI), Utrechtseweg 297, 3731 GA De Bilt, The Netherlands
2  Hydrology and Quantitative Water Management Group, Wageningen University & Research, Wageningen, The Netherlands
3  AgriTech/Mobile for Development, GSM Association (GSMA), London, United Kingdom
4  Department of Water Management, Faculty of Civil Engineering and Geosciences, Delft University of Technology, Delft, The Netherlands
*  Author to whom any correspondence should be addressed.

**E-mail:** aart.overeem@knmi.nl

## Abstract

Commercial microwave links (CMLs) from cellular telecommunication networks can provide a valuable 'opportunistic' source of high-resolution space-time rainfall information, complementing traditional in-situ measurement devices (rain gauges, disdrometers) and remote sensors (weather radars, satellites). Their greatest potential lies in areas with low gauge densities and lack of weather radars, often in developing countries with a subtropical or tropical climate and generally large spatial rainfall variability. Here, the open-source R package RAINLINK is employed to retrieve CML rainfall maps covering the majority of Sri Lanka for a 3.5 month period based on CML data from on average 1140 link paths. These are compared locally to hourly and daily rain gauge data, as well as to rainfall maps from the dual-frequency precipitation radar on board the global precipitation measurement core observatory satellite. The potential of CMLs for real-time tropical rainfall monitoring is demonstrated.

## 1. Introduction

Accurate and timely surface precipitation measurements with high spatial and temporal resolution are of paramount importance for many applications such as water resources management, agriculture (irrigation scheduling and crop insurance) and weather prediction. However, the majority of the Earth's land surface lacks rainfall data of sufficient quality. The total number of rain gauges from operational meteorological networks is estimated to be at most ∼0.25 million, while the number of those giving useful near-real time observations is estimated to be 8000–12 000 (Kidd *et al* 2017). Networks are especially sparse in developing countries (Lorenz and Kunstmann 2012). Moreover, in these areas the coverage of ground-based weather radars is also limited (Saltikoff *et al* 2019). Hence, many regions over the globe (particularly in Africa, South and Southeast

Asia and Latin America) largely depend on satellite-based rainfall observations. Satellite estimates, however, are still associated with large uncertainty and often have a low spatial or temporal resolution (Kidd and Huffman 2011, Li *et al* 2021). Since rainfall displays large variability in space, the current coverage by radars and rain gauges and accuracy of satellites are often not sufficient for many applications such as short-term weather forecasting, flood prediction and water balance monitoring. This calls for alternative sources of near-surface rainfall information to complement the dedicated sensors to improve the quality, spatio-temporal resolution and coverage of quantitative precipitation products. Examples of these alternative sources, also referred to as 'opportunistic sensors', are windshield wipers (Rabiei *et al* 2013), crowdsourced internet of things personal weather stations (De Vos *et al* 2019a), and satellite broadcast receivers (Mercier *et al* 2015). These

sensors—often not even designed to measure rain—fit the rise in demand for environmental opportunistic sensing (Muller *et al* 2015, Zheng *et al* 2018).
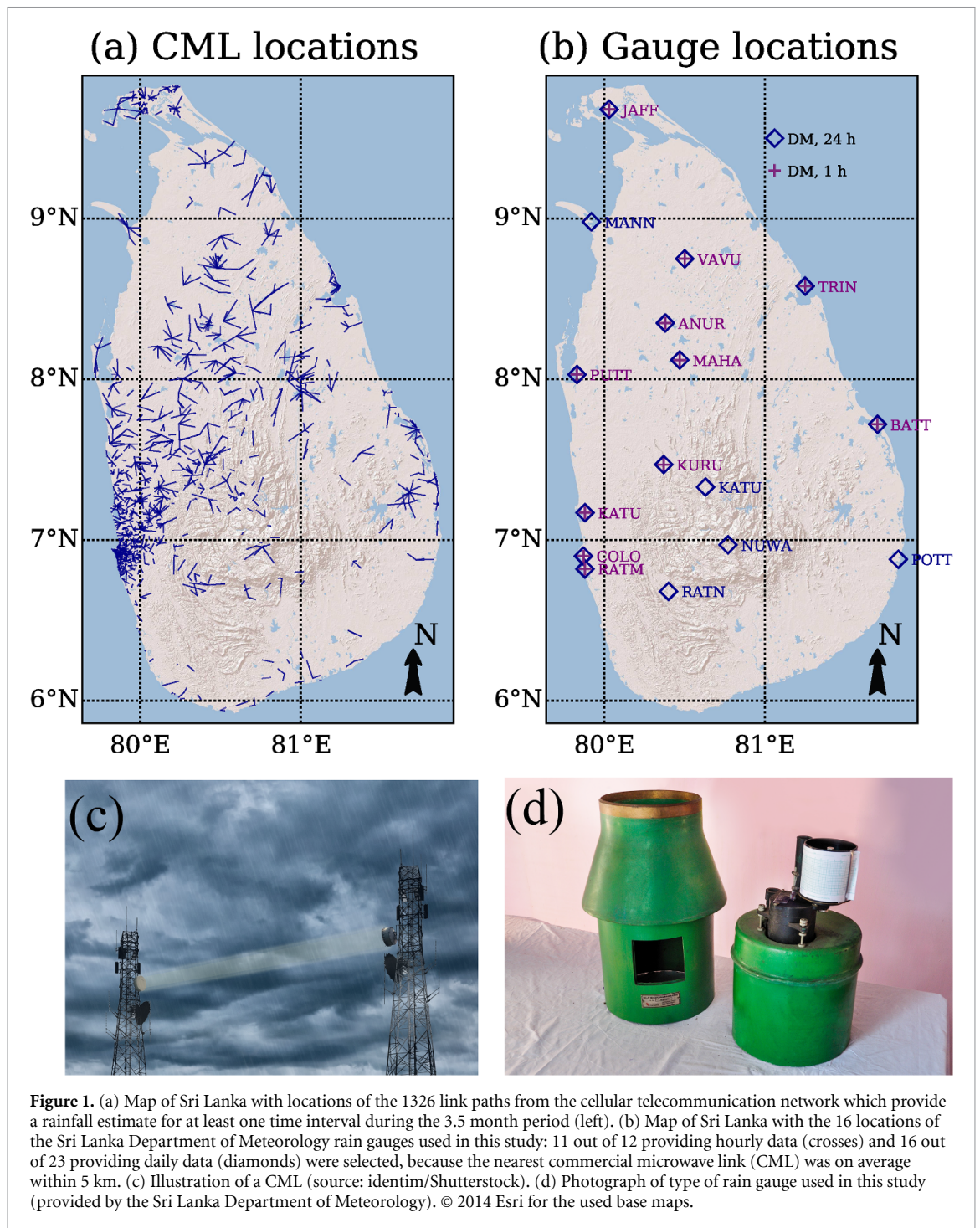
Here, we present one of the most promising sources of opportunistic sensing of rain: commercial microwave links (CMLs), also known as point-to-point or backhaul links. CMLs, called links from now on, are close to the ground radio connections used globally in cellular telecommunication networks. Along such links, radio signals propagate from a transmitting antenna at one base station (radio site, telephone tower or node) to a receiving antenna at another base station (figure 1(c)). A link often consists of multiple sub-links, mainly to allow for communication in both directions. Links operate at frequencies where raindrops substantially attenuate radio waves (Hogg 1968, Atlas and Ulbrich 1977, Olsen *et al* 1978). In rainy circumstances, signals lose their strength as they propagate from a directional antenna on one base station to a directional antenna on another base station within each other's line of sight. This is caused by absorption and scattering of microwaves by raindrops, which have sizes of a few millimeters. Hence, these raindrops are only slightly smaller than the typical wavelength of approximately 1 cm employed by links. The harder it rains, the more raindrops will be present on the path between transmitter and receiver and the larger these drops will be on average. As a consequence, the attenuation of the microwave signal increases with higher rainfall rates.

Rain-induced attenuation and, subsequently, path-averaged rainfall intensity can be retrieved from the signal's attenuation between transmitter and receiver (Upton *et al* 2005, Messer *et al* 2006, Leijnse *et al* 2007a). If transmitted signal levels are constant, the rain-induced attenuation over the link path can be computed by subtracting the received signal level from a reference received signal level, the latter being representative for dry periods. Alternatively, in case of variable transmitted signal levels, the total attenuation over the link path must be used instead of received signal levels. This attenuation is computed by subtracting received signal levels from transmitted signal levels. A reference total attenuation during dry conditions must be computed similarly. Sometimes transmitted signal levels are unknown, but known to be varying; obviously, this method cannot be used in that case. The core of link rainfall retrieval is physics-based and computes the path-averaged rainfall intensity from the rain-induced microwave specific attenuation (dB km$^{-1}$), i.e. the average attenuation per km along a link path due to absorption and scattering of microwaves by rain drops. The relation between the two takes the form of a power-law (Atlas and Ulbrich 1977, Olsen *et al* 1978) of which the coefficients depend mainly on signal frequency and polarization, and are derived from measured rain drop-size distributions and simulations of electromagnetic scattering by rain drops (Leijnse *et al* 2008), preferably for the local climate. Alternatively, the values recommended by Int. Telecommunication Union (2005) can be used as a first guess. The acquired path-averaged rainfall intensities over a link network can subsequently be interpolated to rainfall maps (Overeem *et al* 2013). Comprehensive overviews on the history and physics of link rainfall retrieval have been published (Messer and Sendik 2015, Uijlenhoet *et al* 2018, Chwala and Kunstmann 2019).

We highlight two important sources of error in link rainfall estimation. First, signal levels often decrease during dry periods, e.g. caused by reflection of the beam, dew formation on the antennas, and dust. Wet antennas and strong humidity and temperature gradients in the atmosphere may lead to an altered antenna pattern or to refraction of the beam along the link path (Upton *et al* 2005, Overeem *et al* 2011, Chwala *et al* 2012, Doumounia *et al* 2014, Messer and Sendik 2015). Hence, a reliable classification of wet and dry periods is needed to prevent erroneous rainfall estimates during dry periods (Overeem *et al* 2011, 2016b, Polz *et al* 2020). Moreover, this is also needed to determine a reliable reference signal level, which is representative for dry periods. Here, we apply a method which considers the mutual decrease in received signal levels from surrounding links to determine whether it is raining or not. Second, antennas may also get wet during rain. Hence, a wet antenna attenuation correction is commonly applied, to avoid overestimation due to a water layer on the antenna(s) (Kharadly and Ross 2001, Leijnse *et al* 2007a, 2007b, Schleiss *et al* 2013). Systematic descriptions of encountered sources of error and methods to account for these using quality control and rainfall retrieval algorithms are provided by Overeem *et al* (2016a, 2016b) and Graf *et al* (2020).

Since approximately 2005, a growing community of researchers (Gosset *et al* 2016) has, in close collaboration with mobile network operators, developed retrieval algorithms to convert the raw link signals to rainfall estimates. So far, this has resulted in tens of peer-reviewed scientific publications, which demonstrate the potential of link rainfall monitoring in the Czech Republic (Fencl *et al* 2015), France (Schleiss *et al* 2013), Germany (Chwala *et al* 2012, Graf *et al* 2020), Israel (Messer *et al* 2006, Rayitsfeld *et al* 2012), Italy (Roversi *et al* 2020), the Netherlands (Leijnse *et al* 2007a, Overeem *et al* 2013, 2016b, De Vos *et al* 2019b), and Switzerland (Bianchi *et al* 2013a). A key advantage is that the required infrastructure is already in place, in the form of the ∼5 million links in global use (Ericsson 2018) by mobile network operators, who typically store the required signal level data in their network management systems to monitor network stability. Typically, minimum and maximum, average, or instantaneous received signal level data are stored every 15 min.

**Figure 1.** (a) Map of Sri Lanka with locations of the 1326 link paths from the cellular telecommunication network which provide a rainfall estimate for at least one time interval during the 3.5 month period (left). (b) Map of Sri Lanka with the 16 locations of the Sri Lanka Department of Meteorology rain gauges used in this study: 11 out of 12 providing hourly data (crosses) and 16 out of 23 providing daily data (diamonds) were selected, because the nearest commercial microwave link (CML) was on average within 5 km. (c) Illustration of a CML (source: identim/Shutterstock). (d) Photograph of type of rain gauge used in this study (provided by the Sri Lanka Department of Meteorology). © 2014 Esri for the used base maps.

Currently, link rainfall estimation has been primarily demonstrated for temperate and Mediterranean climates, with generally reasonable coverage by dedicated sensors. Datasets with a few thousand links were analyzed over a 2.5 year (Overeem *et al* 2016b) and a 1 year period (Graf *et al* 2020) over the Netherlands and Germany, respectively. However, the greatest potential of link rainfall estimation is in low- and middle-income countries with subtropical or tropical climates, with limited real-time rainfall observations to capture the typical localized and intense rain showers. Rain gauge data will not always

be automatically disseminated. For instance, charts from the self-recording pluviographs in Sri Lanka, used in this study, need to be manually read and digitized. Only few studies address link rainfall estimation in these regions. Good performance is found by Doumounia *et al* (2014) for one sub-link in Burkina Faso over a 2 month period and by Sohail Afzal *et al* (2018) for 35 sub-links in Pakistan over a 55 day period. Hoedjes *et al* (2014) show a rainfall map based on data from six sub-links in Kenya and compare it to a map of satellite brightness temperatures. Rios Gaona *et al* (2018) provide rainfall estimates for

Brazil, based on 145 sub-links (95 link paths) over 81 days. City-average rainfall dynamics for São Paulo were captured, but mixed results were obtained for individual link estimates. Finally, pilot studies have been performed in Nigeria and Sri Lanka (GSM Association 2019).

To assess the potential of links for rainfall monitoring in tropical regions a thorough evaluation on much larger datasets is required. We contribute to this by employing the open-source R package RAINLINK (2020) to retrieve rainfall in Sri Lanka, a middle-income country. Rainfall in Sri Lanka's central mountains is important for hydropower and the tea industry. The quality of tea is influenced by rainfall amount, intensity and duration (Herath and Ratnayake 2004). Furthermore, strong seasonal and spatial rainfall variability creates periodic water shortages for irrigated agriculture and households. Both rainfed and irrigated agriculture is important for exports for Sri Lanka. Understanding spatio-temporal rainfall variability and improving rainfall forecasts may help in, for example, planning crop cultivation and drainage channels for flood mitigation, or in designing water storages (Jayawardene *et al* 2005). Here, we employ link data from, on average, 1140 link paths over a 3.5 month period. Link rainfall maps are compared to hourly and daily rainfall depths from 11 and 16 official meteorological stations, respectively. Given the absence of weather radars and the limited quality of many satellite precipitation products, for the first time link rainfall maps are compared to those from the Dual-frequency Precipitation Radar on board the global precipitation measurement (GPM) core observatory satellite (Hou *et al* 2014, Skofronick-Jackson *et al* 2017, 2018) for 12 events. This active satellite sensor will generally provide much better rainfall estimates than those from passive satellite-based sensors, although its temporal coverage is limited. Note that GPM is the successor of the tropical rainfall measurement mission building upon its legacy of precipitation estimation from space from 1997 to 2015 (Liu *et al* 2012, NASA 2021a, 2021b).

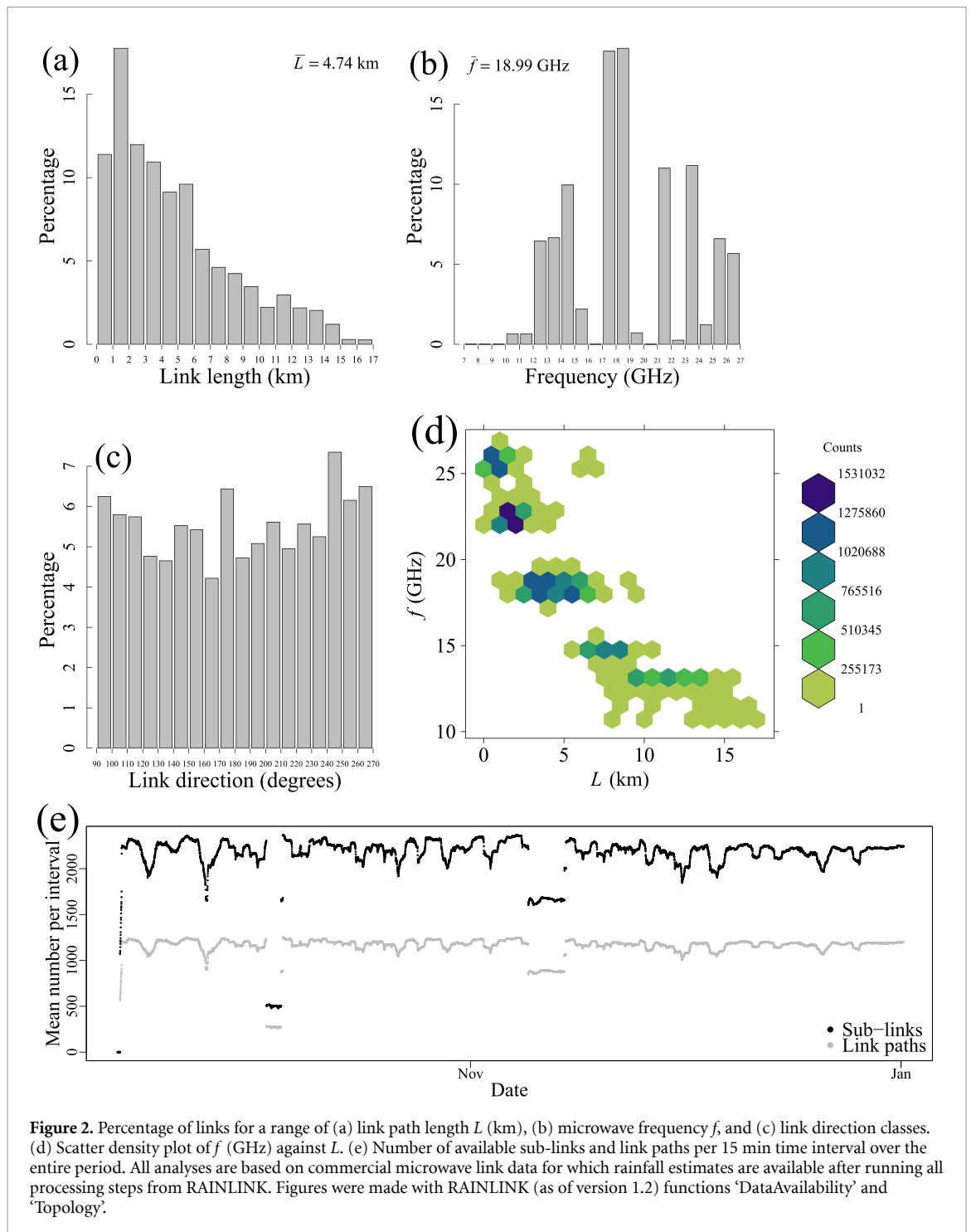## 2. Data

### 2.1. Study area
Sri Lanka (65 610 km$^2$; ∼22 million inhabitants) is an island country in the Indian Ocean, located in South Asia near the equator, southeast of India (figure 1(a)). It has a warm tropical monsoon climate tempered by ocean winds and considerable moisture, with an average annual temperature of about 27°C in the lowlands. Steep orography is found in the mountain massif in the south central part with a highest peak of ∼2500 m above m.s.l. The rest of Sri Lanka is typically up to a few hundred meters above m.s.l. Mean annual rainfall varies from below 900 mm (southeast and northwest) to over 5000 mm

(western slopes of mountain massif). Monsoon winds from the Indian Ocean and Bay of Bengal, orography, and migrations of the intertropical convergence zone cause strong seasonal variation in rainfall. About 20% of the land surface is in the wet zone (>2500 mm), the rest is in the intermediate (1750–2500 mm) and dry (900–1750 mm) zones (Malmgren *et al* 2003, Herath and Ratnayake 2004, Nisansala *et al* 2020, Sri Lanka Department of Meteorology 2020).

The period we consider in this study runs from 12 September to 31 December 2019. The period from 12 to 30 September falls within the Southwest Monsoon (May–September), during which moisture from the Indian Ocean brings 100–3000 mm of rainfall. Rainfall is high in the southwest of the island and on the windward mountain slopes, with the latter receiving up to 2500 mm per month. Leeward slopes in the east and northeast receive little rain. This is followed by the second intermonsoon from October through November, when the intertropical convergence zone migrates southward over Sri Lanka. High-intensity rainfall events as well as the associated influence of large-scale weather systems (such as tropical depressions and cyclones originating in the Bay of Bengal) are common. Such weather systems lead to strong winds with widespread rain over the whole of Sri Lanka, which can sometimes result in floods and landslides. Almost all of Sri Lanka experiences over 400 mm of rain in this period, with the southwestern slopes obtaining 750–1200 mm. This is followed by the Northeast Monsoon which runs from December through to February and is accompanied by dry and cold winds from India and monsoon winds from the northeast, which bring moisture from the Bay of Bengal. Rainfall amounts vary in space from 177 mm for the western coastal area to 1250 mm for the northeastern slopes of the mountains (Malmgren *et al* 2003, Herath and Ratnayake 2004, Nisansala *et al* 2020, Sri Lanka Department of Meteorology 2020).

### 2.2. Commercial microwave link data
Minimum and maximum received signal levels over 15 min intervals were obtained for the period from 12 September to 31 December 2019, from part of the cellular telecommunication network operated by mobile network operator Dialog Sri Lanka, covering the majority of Sri Lanka. Figure 1(a) shows the locations of the 1326 link paths for which rainfall estimates are obtained. Information on link path length $L$, employed microwave frequency $f$ and link orientation is presented in figures 2(a)–(c). The majority of links is shorter than 5 km, the average link path length being 4.7 km. Most links operate at frequencies between 17 and 19 GHz. The orientation of links is quite uniformly distributed over all directions. The employed carrier frequency decreases for increasing link path lengths (figure 2(d)), because link networks have been designed to prevent signal loss and lower

**Figure 2.** Percentage of links for a range of (a) link path length $L$ (km), (b) microwave frequency $f$, and (c) link direction classes. (d) Scatter density plot of $f$ (GHz) against $L$. (e) Number of available sub-links and link paths per 15 min time interval over the entire period. All analyses are based on commercial microwave link data for which rainfall estimates are available after running all processing steps from RAINLINK. Figures were made with RAINLINK (as of version 1.2) functions 'DataAvailability' and 'Topology'.

frequencies are less affected by attenuation. Higher carrier frequencies are generally used in (urban) areas where more bandwidth is needed. Frequencies are generally lower compared to those in areas with a temperate climate, in order to prevent signal loss due to the more intense tropical rainfall. Figure 2(e) shows that the mean 15 min data availability varies in time, but is generally high. Rainfall estimates have been provided for, on average, 2134 sub-links and 1140 link paths (this is less than the 1326 link paths for which data are available due to filtering we apply on these data) over the 3.5 month period.

Link metadata are coupled with signal level data and an initial quality control is performed. Overeem *et al* (2016a) give a detailed description of the employed rainfall retrieval algorithm, the interpolation methodology and the implementation thereof in the RAINLINK software package, written in scripting language R. Version 1.2 is used to retrieve 15 min path-averaged rainfall intensities, which are subsequently interpolated to 15 min rainfall maps on a 0.02° (~4 km²) grid. These are aggregated to hourly rainfall maps and to daily rainfall maps from 08:30 to 08:30 local time (03:00 UTC) to match the

measurement interval of rain gauges. RAINLINK's default parameter settings (Overeem *et al* 2016a) are employed. Although these have been optimized for the Netherlands, which has a temperate climate, we expect that these settings will yield acceptable rainfall estimates. The entire processing chain is described in the supporting information (text S1) (available online at stacks.iop.org/ERL/16/074058/mmedia).

### 2.3. Rain gauge data
Hourly and daily rain gauge data were obtained from the Sri Lanka Department of Meteorology for, respectively, 12 and 23 locations. Only those World Meteorological Organization stations were selected for which the average distance to the nearest antenna of a link that has data available was within 5 km during the 3.5 month period considered. This resulted in a selection of 11 gauges with hourly rainfall depths and 16 gauges with daily rainfall depths (figure 1(b)). The data are from a siphon type of rain gauge, where a pluviograph was employed for recording the hourly rainfall depths. The daily rainfall depths were obtained from the same gauge by accumulating 3-h rainfall depths, which were measured manually every 3 hours starting from 08:30 local time to the next day 08:30 local time (∼96% availability). A manual observation was performed by emptying the gauge in a measuring glass. The average availability of hourly rainfall depths is lower due to mechanical problems (85%).

### 2.4. Satellite product
The satellite-based precipitation estimates were retrieved from GPM's combined precipitation product (based on the GPM Combined Radar-Radiometer Precipitation Algorithm, version V06A). Within this dataset, precipitation retrieval is based on both the radiometer and the dual-frequency precipitation radar onboard the core observatory satellite, which has roughly one overpass per day for a given location. This precipitation product distinguishes precipitation retrieval based on the frequency band used for retrieval. The normal swath is based on the Ku-band radar and has a wider scan range compared to the matched scan in which data from the Ku- and Ka-band radar is combined. Because of its wider swath, precipitation estimates from the normal swath were used in this study as we wanted to compare as many events as possible. More information about this dataset can be found in Grecu *et al* (2016), Olson and the GPM Combined Radar-Radiometer Algorithm Team (2018). All swaths covering Sri Lanka within the study period were analyzed and only those for which at least one pixel over the land surface of Sri Lanka had surface precipitation $>0$ mm h$^{-1}$ were considered for further analysis. This results in a selection of 12 events for which both satellite and link data were available. Data from the selected events were interpolated (using bilinear interpolation) to match the link grid in order to compare the satellite and link precipitation retrievals.

## 3. Results
Figure 3 shows the cumulative daily rainfall depths from links and gauges from 12 September until 31 December 2019, the period being shorter in case of missing rain gauge data. Note that cumulative rainfall can easily exceed 800 mm in 3.5 months, and can even exceed 1500 mm. The variation with time of the rainfall depths from links and gauges agree reasonably well. The magnitude is in good agreement for six locations, reveals overestimation for one location, underestimation for four locations, and severe underestimation for five locations.

A more quantitative evaluation is provided by the scatter plots of link hourly and daily rainfall depths against the gauge-based ones (figure 4). A slight overestimation by links is found for hourly rainfall, whereas for daily rainfall the average underestimation is 17.6%. This is probably caused by differences in availability and collection of hourly and daily gauge data. The coefficient of determination ($r^2$; the fraction of explained variance) is fairly large (0.57), although quite some scatter is found, as is confirmed by the coefficient of variation (CV) of the residuals of 4.33. Here, the CV is defined as the ratio of the standard deviation of the residuals and the mean of the reference. This scatter and the apparent large link rainfall depths for (near) zero gauge rainfall (false alarms) can be a result of errors in link rainfall retrievals, but may also be related to the interplay between strong spatial rainfall variability and differences in link and gauge locations. Furthermore, gauge rainfall estimates themselves are influenced by sources of error. Except for the underestimation, link rainfall estimates vastly improve for daily rainfall ($r^2 = 0.79$ and CV $= 0.87$), where spatial rainfall variability is generally much smaller, such that differences in locations between links and gauges are expected to play much less of a role. It is remarkable that links can even accurately capture daily rainfall depths over 150 mm.

Finally, 15 min link rainfall maps are compared to the satellite product for 12 events (figure 5). In most cases the locations of rain areas agree reasonably well. One of the best matches is found for 17 October 2019 (figure 5(e)): The entire event of link rainfall maps is provided as supporting information (movie S1) and shows realistic patterns of showers moving across Sri Lanka during this Second Intermonsoon. Link and satellite rainfall maps may differ because the satellite only takes a snapshot during its overpass, and hence does not provide an estimate for the entire 15 min interval. Moreover, low link network density
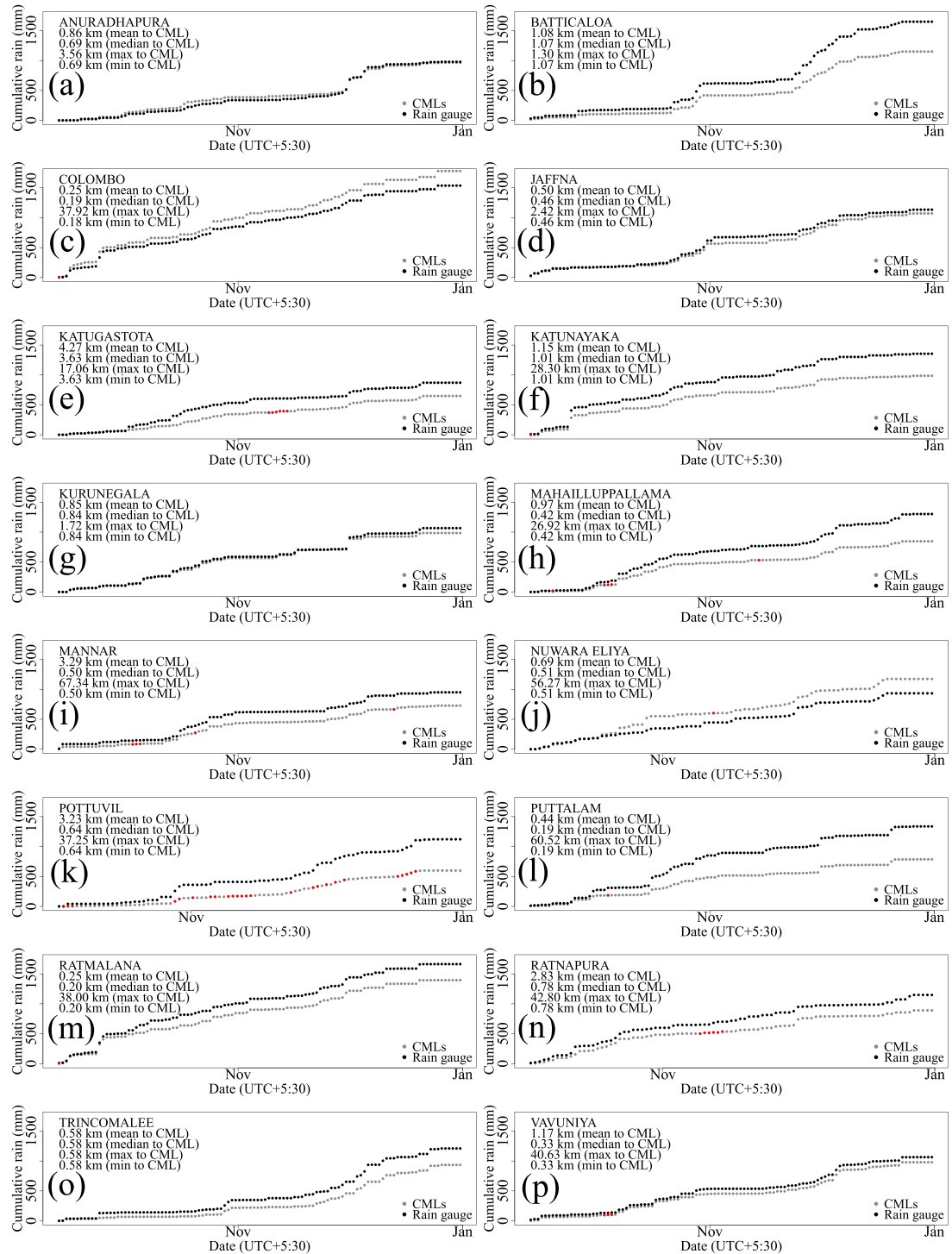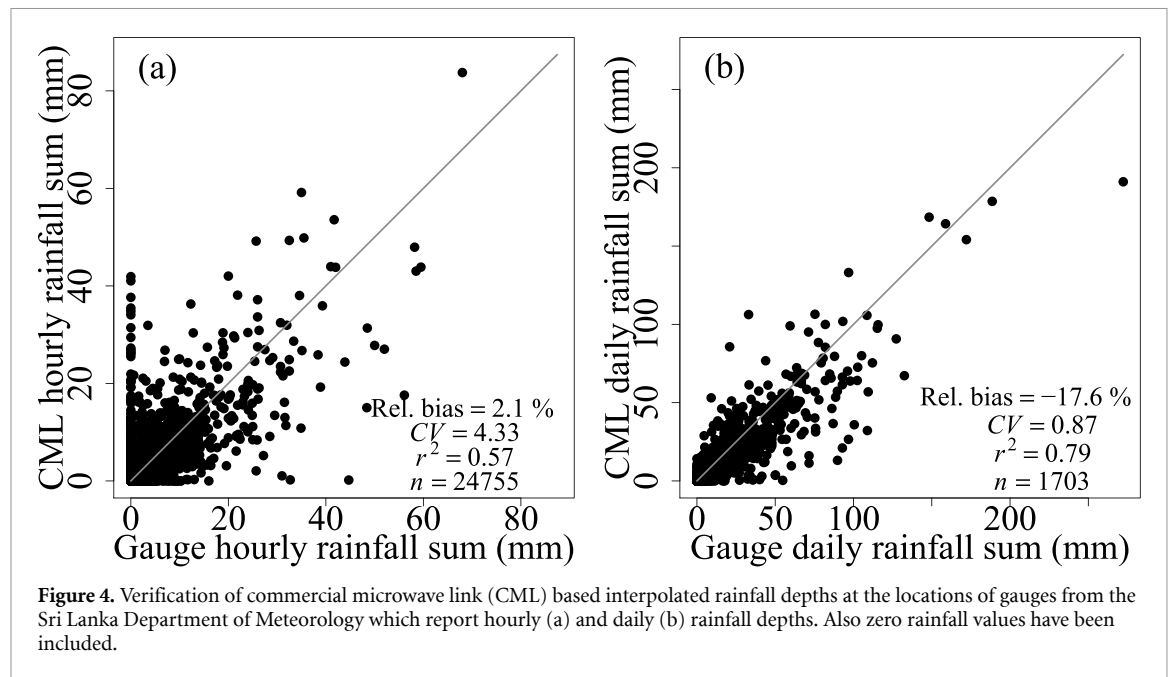
**Figure 3.** (a)–(p) Cumulative rainfall depths. Comparison of commercial microwave link (CML) based daily interpolated rainfall depths at the locations of gauges from the Sri Lanka Department of Meteorology which report daily rainfall depths. The red dots indicate the days for which the maximum distance of the underlying 15 min data to the nearest link antenna is larger than 5 km, and hence could have been large during rainfall.

in some areas may lead to lower-quality link rainfall estimates.

## 4. Discussion

It is rather speculative what causes differences in performance among gauge stations (figure 3). Only for

one location the large distance (indicated by the red dots in figure 3(k)) between the gauge and the nearest link may have contributed to link rainfall underestimation. Although differences in distance to the nearest link do not seem to provide an explanation, link network density could differ between rain gauge locations. Higher densities could capture local extremes

**Figure 4.** Verification of commercial microwave link (CML) based interpolated rainfall depths at the locations of gauges from the Sri Lanka Department of Meteorology which report hourly (a) and daily (b) rainfall depths. Also zero rainfall values have been included.

more accurately. Possibly some locations have shorter link paths, which may negatively affect results (De Vos *et al* 2019b). Differences between link and gauge rainfall estimates in figures 3 and 4 may also be caused by sources of error in gauge rainfall observations, which may vary between gauge locations. For instance, daily rainfall depths are based on eight manual observations and can hence be affected by reading errors. Rain gauges can malfunction due to dirt (Steiner *et al* 1999) and turbulence can lead to undercatch (Pollock *et al* 2018). A more extensive reference network would be needed in order to draw more definite conclusions regarding link-gauge differences.

When only gauge estimates above 1 mm are considered (i.e. a subset of figure 4), an underestimation of 15.6%, a $r^2$ of 0.58 and a much better CV of 0.86 is found for hourly rainfall (1422 values). For daily values over 1 mm we find an underestimation of 18.6%, a worse $r^2$ of 0.75 and a better CV of 0.63 (929 values). This performance for daily rainfall above 1 mm is better than what was found for the Netherlands ($\sim$35 000 km$^2$), except for the stronger underestimation: Overeem *et al* (2016b) report an underestimation of 7.8%, a $r^2$ of 0.59 and a CV of 0.67. This is based on rainfall maps from a dense link network spanning about 7 summer months, with a gauge-adjusted radar rainfall dataset as reference. The current results are quite remarkable since RAINLINK's parameters have not been optimized for the Sri Lankan climate. We think this can be partly explained by the generally higher rainfall intensities in Sri Lanka. Then the influence of wet antenna attenuation and errors in wet-dry classification will be relatively small. Still, it is recommended to customize the rainfall retrieval algorithm settings for local

climate and network conditions instead of using the parameter values found for the Netherlands, which has a temperate climate. This customization concerns the core of the algorithm: the coefficients of the power-law between path-average rainfall intensity and specific attenuation, and the mixing of minimum and maximum received signals to derive average rainfall intensities. The power-law coefficient and exponent for a given microwave frequency are derived from measured rain drop-size distributions and simulations of electromagnetic scattering by rain drops (Leijnse *et al* 2008). This requires drop-size distribution measurements from the considered region or a similar climate. The relative contribution of the minimum and maximum received signals depend on the probability density function of path-averaged rainfall intensities typical for the region. This parameter can hence be derived from such probability density information, but also by means of a statistical calibration by comparing to a reference dataset (Overeem *et al* 2016a, De Vos *et al* 2019b). Such a calibration can also be used to optimize other parameters for the region, preferably by using a stochastic optimization that optimizes RAINLINK's most important parameters for wet-dry classification and rainfall retrieval separately (Wolff *et al* 2021).

Messer and Sendik (2015), Uijlenhoet *et al* (2018) and Chwala and Kunstmann (2019) provide detailed discussions on (the sources of error of) different rainfall retrieval and mapping algorithms, where Overeem *et al* (2016a, 2016b) specifically focus on RAINLINK and its applicability. To gain a better understanding of differences between link and reference data, notably the underestimations in cumulative rainfall against gauges for several locations, would
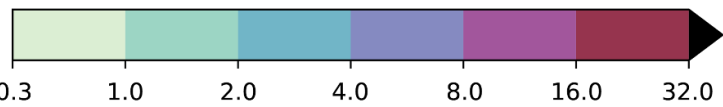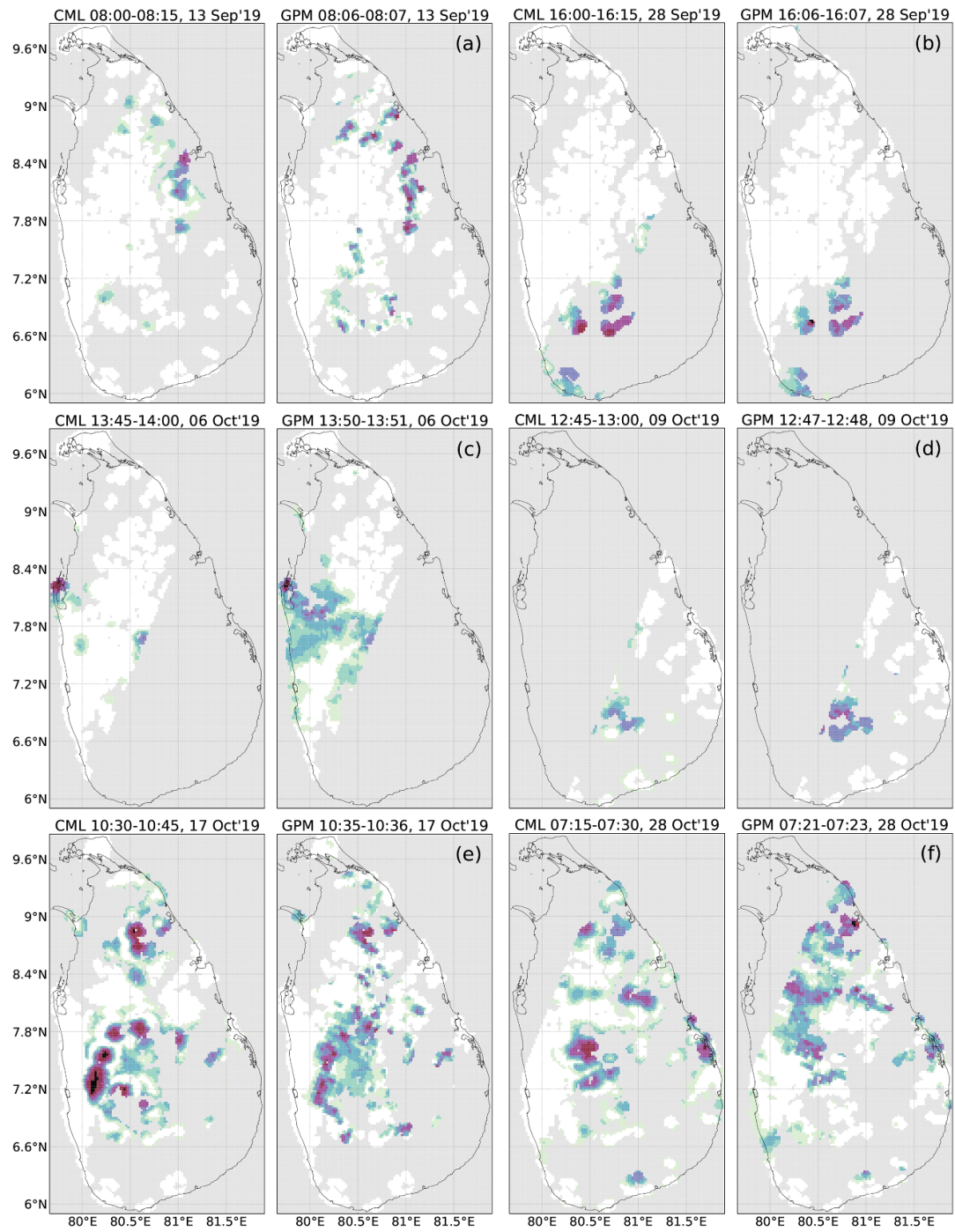
**Figure 5.** (a)–(l) Comparison of commercial microwave link (CML) based 15 min rainfall maps (left) versus those from a satellite product, the GPM combined precipitation product (based on the GPM Combined Radar-Radiometer Precipitation Algorithm, version V06A; right) for 12 rainfall events over Sri Lanka from 2019 (two panels per event). For the rainfall event on 17 October (e) a movie is provided in the supporting information (movie S1). Time is in UTC. Only areas with combined satellite and link coverage are plotted, the latter implying that the nearest link antenna is within ∼5 km for the given time interval. White areas denote a rainfall intensity less than 0.3 mm h$^{-1}$. Grey areas do not have combined satellite and link coverage.
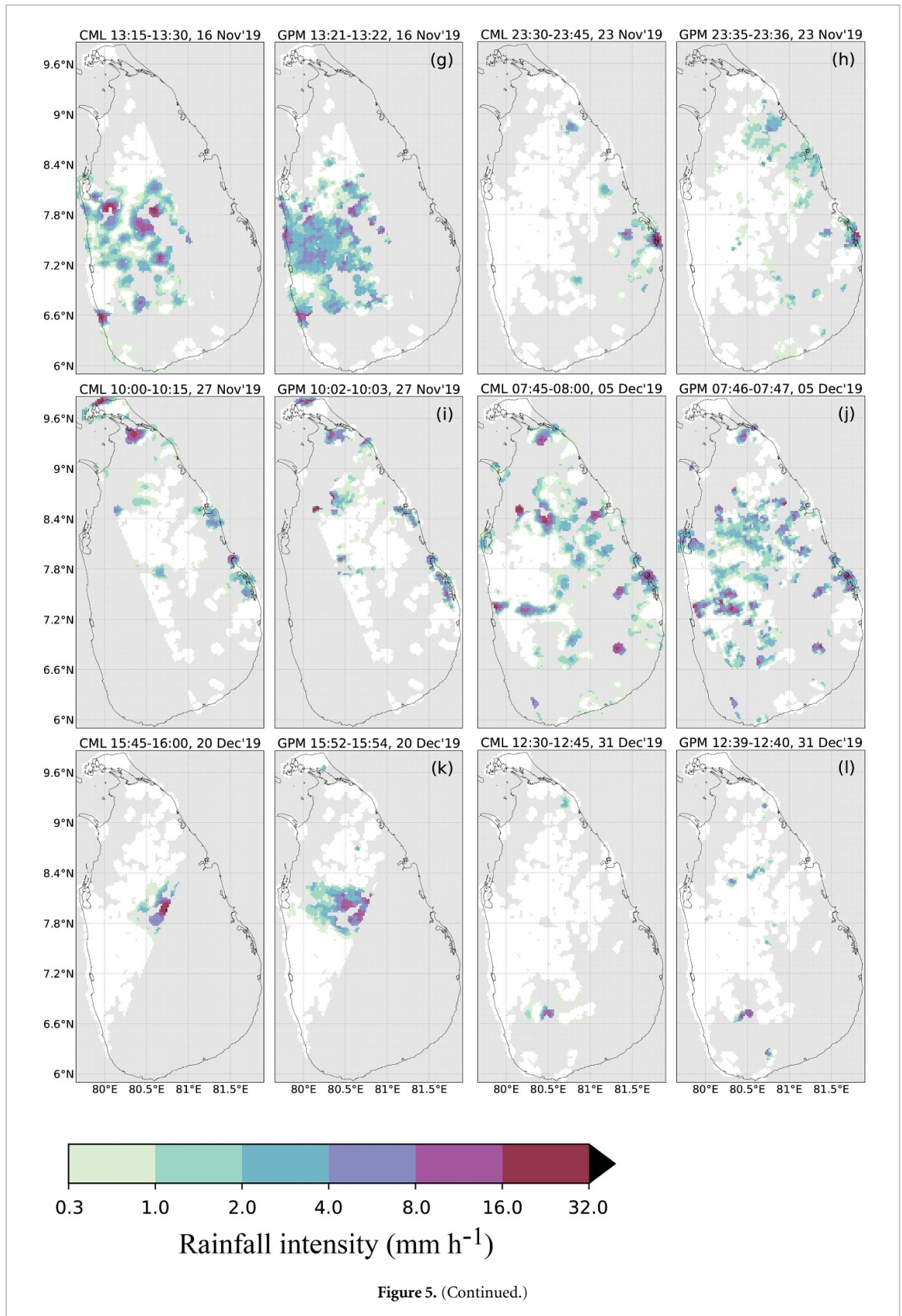
**Figure 5.** (Continued.)

require a detailed study of sources of error. This could be accomplished by employing local weather station data and a dedicated research experiment with rain gauges and disdrometers (instruments that measure raindrop size distributions) along a link path combined with time lapse cameras to monitor the link antennas and the link path (Van Leth *et al* 2018). Such an experiment would also provide opportunities to improve link rainfall retrieval algorithms (Wang *et al* 2012).

## 5. Conclusions

These are the main conclusions from this study:

- An unprecedented CML dataset in terms of spatial and temporal coverage was used for rainfall mapping in the tropical country Sri Lanka.
- A spatial comparison with a high-quality satellite product (Grecu *et al* 2016) and an extensive local comparison with rain gauge data confirms the potential of microwave links for detailed tropical rainfall monitoring over land.
- The density of the link network is generally much higher than that of gauge networks providing sub-daily data. For example, the Sri Lanka Department of Meteorology operates 23 official meteorological stations providing hourly rainfall for the entire country, whereas data from, on average, 1140 link paths were available in this study. This is only part of the network of one of the mobile network operators active in Sri Lanka.

## 6. Outlook

Only satellites can provide precipitation information on a global basis, albeit with issues concerning accuracy (Kidd and Huffman 2011). For instance, the IMERG product of the GPM mission is a gridded rainfall dataset covering 60° N–60° S with a spatial resolution of 0.1° and an interpolated temporal resolution of 30 min (Hou *et al* 2014). This coverage cannot be achieved with CML, rain gauge or radar networks, also because they are virtually absent above the 71% Earth's surface consisting of oceans. The advantage of cellular telecommunication networks is that they are ubiquitous in populated areas, covering more than 90% of the world's population (International Telecommunication Union 2020). In 2007, already 20% of the Earth's land surface was covered by cellular telecommunication networks (GSM Association 2012). Hence, CMLs in these networks could provide accurate and much more detailed rainfall information in populated areas, where the impact of severe weather is expected to be largest.

Links are a complementary source of rainfall information and are not meant to replace existing observational networks. Once the quality of link rainfall estimates has been established for a certain region, these are ultimately merged with rainfall products from dedicated sensor networks (Grum *et al* 2005, Overeem *et al* 2012, Bianchi *et al* 2013b, Haese *et al* 2017). For developing countries in subtropical and tropical areas, link and satellite rainfall products could be merged. In these areas, the high spatio-temporal resolution and accuracy of links is unmatched, complementing the large coverage of satellites. Rios Gaona *et al* (2017) evaluate the IMERG product of the GPM mission, two geostationary rainfall products and link-based rainfall estimates against a gauge-adjusted radar rainfall dataset over the Netherlands. The 7 month evaluation shows that links outperform satellite rainfall products, highlighting the potential for improving satellite products through merging with link rainfall estimates.

A number of hurdles have to be overcome before (merged) link rainfall products can be used operationally. First, gaining access to link data is usually difficult and is typically achieved by contacting mobile network operators on a country-by-country basis. Here, we obtained link data from Sri Lanka by the active involvement of the Mobile for Development AgriTech program of the GSM Association. The GSMA represents the interests of mobile network operators worldwide. Ideally, link data should be openly available to enable the development of rainfall products. Support from the World Meteorological Organization, the International Telecommunication Union, space agencies, meteorological satellite agencies and policy makers could foster this.

Second, several technical issues need to be addressed. Metadata (comprising link locations, lengths, frequencies, polarizations, etc) are often not present in the link data files, while such data are crucial in converting link data to rain estimates. Coupling of available metadata to the data files is challenging and time-consuming because of large variation of storing metadata between mobile network operators, and the sometimes ambiguous or missing information therein. This calls for standardization of link (meta)data at the link vendor level, for which the preliminary HDF5 data format standard 'cmlh5' could be used as a starting point (cmlh5 2020). Additionally, the data management of mobile network operators is not geared toward (continuous real-time) delivery of link data to other parties. Ultimately, an application programming interface (API) should be developed which can handle link data acquisition, the coupling of data and metadata, the rainfall retrieval and the dissemination of rainfall information. Implementing an open source data acquisition system may help to gain link data more easily and would increase control of the involved sampling up to 1 s (Chwala *et al* 2016).

Third, in order to perform a thorough scientific evaluation of their performance, rainfall retrievals from the typically hundreds to thousands links from preferably one or more years need to be evaluated for each network and region. Also, initial quality control of (meta)data may be needed. This requires good reference data, which are especially scarce in subtropical and tropical areas. A satellite combined radar-radiometer product provides a means to perform a spatial comparison, but typically only once a day. Also customizing retrieval and mapping parameters to the local climate and network is recommended, although we have shown here that using standard parameters derived for a very different region (the Netherlands) yields remarkably good rainfall estimates.

Fourth, business models need to be developed. Link data will feed into a range of applications, from improving and localizing weather forecasting services, early warnings (e.g. landslides), crop production monitoring, precision agriculture services, agricultural weather insurance and water management. For example, this data will allow national meteorological services or private weather companies to accurately nowcast rainfall up to a few hours in advance, which is currently not feasible given the absence of weather radars. Imhoff *et al* (2020) use link rainfall maps as input for the open-source algorithm pySTEPS and demonstrate that link rainfall nowcasts compare well to radar rainfall nowcasts over the Netherlands. In addition, engineering companies and water authorities could use these data to improve (flash) flood forecasts (Brauer *et al* 2016). Weather micro-insurance products, specifically rainfall excess insurance, can be developed to cater to the predominantly smallholder farming systems found in low- and middle-income countries. These applications present opportunities for mobile network operators to valorize their link data, either as a 'data as a service' product, or by co-developing the above-mentioned services with relevant partner organizations, where other mobile network operator assets, such as delivery channels, location data, and mobile money channels facilitate the creation of such services (GSM Association 2019, 2021). This is also confirmed by the demonstrator project Microwave-based Environmental Monitoring (MEMO 2020) from the Swedish Meteorological and Hydrological Institute and Ericsson, demonstrating live link-based rainfall maps for Gothenburg and Stockholm (Sweden).

To conclude, we hope that this study contributes to enable real-time link rainfall monitoring, especially in those subtropical and tropical regions around the world with few surface rainfall observations.

## Data availability statement

The satellite product, the global precipitation measurement (GPM) combined (CMB) precipitation product (based on the GPM Combined Radar-Radiometer Precipitation Algorithm, version V06A), can be freely obtained via https://gpm.nasa.gov/data/directory. The gridded rainfall maps retrieved from CML data from Sri Lanka over the 3.5 month period can be freely obtained (Overeem 2021). The data generated and/or analysed during the current study are not publicly available for legal/ethical reasons but are available from the corresponding author on reasonable request.

## ORCID iDs

Aart Overeem ⦿ https://orcid.org/0000-0001-5550-8141
Hidde Leijnse ⦿ https://orcid.org/0000-0001-7835-4480
Thomas C van Leth ⦿ https://orcid.org/0000-0003-1597-6041
Linda Bogerd ⦿ https://orcid.org/0000-0002-7343-4542
Arjan Droste ⦿ https://orcid.org/0000-0003-0218-5160
Remko Uijlenhoet ⦿ https://orcid.org/0000-0001-7418-4445

## References

Atlas D and Ulbrich C W 1977 Path- and area-integrated rainfall measurement by microwave attenuation in the 1–3 cm band *J. Appl. Meteorol.* **16** 1322–31

Bianchi B, Rieckermann J and Berne A 2013a Quality control of rain gauge measurements using telecommunication microwave links *J. Hydrol.* **492** 15–23

Bianchi B, van Leeuwen P J, Hogan R J and Berne A 2013b A variational approach to retrieve rain rate by combining information from rain gauges, radars and microwave links *J. Hydrometeorol.* **14** 1897–909

Brauer C C, Overeem A, Leijnse H and Uijlenhoet R 2016 The effect of differences between rainfall measurement techniques on groundwater and discharge simulations in a lowland catchment *Hydrol. Process.* **30** 3885–900

Chwala C *et al* 2012 Precipitation observation using microwave backhaul links in the alpine and pre-alpine region of Southern Germany *Hydrol. Earth Syst. Sci.* **16** 2647–61

Chwala C, Keis F and Kunstmann H 2016 Real-time data acquisition of commercial microwave link networks for hydrometeorological applications *Atmos. Meas. Tech.* **9** 991–9

Chwala C and Kunstmann H 2019 Commercial microwave link networks for rainfall observation: assessment of the current status and future challenges *WIREs Water* **6** e1337

cmlh5 2020 Github–cmlh5/cmlh5: a file format for commercial (and other) microwave link data based on HDF5 (available at: https://github.com/cmlh5/cmlh5) (Accessed 30 December 2020)

De Vos L W, Leijnse H, Overeem A and Uijlenhoet R 2019a Quality control for crowdsourced personal weather stations to enable operational rainfall monitoring *Geophys. Res. Lett.* **46** 8820–9

De Vos L W, Overeem A, Leijnse H and Uijlenhoet R 2019b Rainfall estimation accuracy of a nationwide instantaneously sampling commercial microwave link network: error dependency on known characteristics *J. Atmos. Ocean Technol.* **36** 1267–83

Doumounia A, Gosset M, Cazenave F, Kacou M and Zougmore F 2014 Rainfall monitoring based on microwave links from cellular telecommunication networks: first results from a West African test bed *Geophys. Res. Lett.* **41** 6016–22

Ericsson 2018 Ericsson microwave outlook (available at: www.ericsson.com/4a312c/assets/local/ reports-papers/microwave-outlook/2018/ericsson-microwave-outlook-report-2018.pdf) (Accessed 10 June 2021)

Fencl M, Rieckermann J, Sýkora P, Stránský D and Bareš V 2015 Commercial microwave links instead of rain gauges: fiction or reality? *Water Sci. Technol.* **71** 31–7

Gosset M *et al* 2016 Improving rainfall measurement in gauge poor regions thanks to mobile telecommunication networks *Bull. Am. Meteorol. Soc.* **97** ES49–ES51

Graf M, Chwala C, Polz J and Kunstmann H 2020 Rainfall estimation from a German-wide commercial microwave link network: optimized processing and validation for 1 year of data *Hydrol. Earth Syst. Sci.* **24** 2931–50

Grecu M, Olson W S, Munchak S J, Ringerud S, Liao L, Haddad Z, Kelley B L and McLaughlin S F 2016 The GPM combined algorithm *J. Atmos. Ocean Technol.* **33** 2225–45

Grum M, Kraemer S, Verworn H-R and Redder A 2005 Combined use of point rain gauges, radar, microwave link and level measurements in urban hydrological modelling *Atmos. Res.* **77** 313–21

GSM Association 2012 Universal access. How mobile can bring communications to all (available at: www.gsma.com/publicpolicy/wp-content/uploads/ 2012/03/universalaccessfullreport.pdf) (Accessed 10 June 2021)

GSM Association 2019 Mobile technology for rural climate resilience: the role of mobile operators in bridging the data gap (available at: www.gsma.com/mobilefordevelopment/ wp-content/uploads/2019/10/GSMA_AgriTech_Climate _Report.pdf) (Accessed 10 June 2021)

GSM Association 2021 Digital innovation for climate-resilient agriculture: using rainfall data from mobile networks for localised and scalable services (available at: www.gsma.com/ mobilefordevelopment/wp-content/uploads/2021/03/ Digital_Innovation_for_Climate_Resilient_Agriculture.pdf) (Accessed 10 June 2021)

Haese B, Hörning S, Chwala C, Bárdossy A, Schalge B and Kunstmann H 2017 Stochastic reconstruction and interpolation of precipitation fields using combined information of commercial microwave links and rain gauges *Water Resour. Res.* **53** 10740–56

Herath S and Ratnayake U 2004 Monitoring rainfall trends to predict adverse impacts—a case study from Sri Lanka (1964–1993) *Glob. Environ. Change* **14** 71–9

Hoedjes J C B *et al* 2014 A conceptual flash flood early warning system for Africa, based on terrestrial microwave links and flash flood guidance *ISPRS. Int. J. Geo-Inf.* **3** 584–98

Hogg D 1968 Millimeter-wave communication through the atmosphere *Science* **159** 39–46

Hou A Y, Kakar R K, Neeck S, Azarbarzin A A, Kummerow C D, Kojima M, Oki R, Nakamura K and Iguchi T 2014 The global precipitation measurement mission *Bull. Am. Meteorol. Soc.* **95** 701–22

International Telecommunication Union 2020 Measuring digital development - Facts and figures 2020, Geneva, Switzerland (available at: www.itu.int/en/ITU-D/Statistics/Documents/ facts/FactsFigures2020.pdf")

Imhoff R O, Overeem A, Brauer C C, Leijnse H, Weerts A H and Uijlenhoet R 2020 Rainfall nowcasting using commercial microwave links *Geophys. Res. Lett.* **47** e2020GL089365

Int. Telecommunication Union 2005 Recommendation ITU-R P.838-3. Specific attenuation model for rain for use in prediction methods (available at: www.itu.int/dms_pu-brec/itu-r/rec/p/R-REC-P.838-3-200503-I!!PDF-E.pdf) (Accessed 30 December 2020)

Jayawardene H, Sonnadara D and Jayewardene D 2005 Trends of rainfall in Sri Lanka over the last century *Sri Lankan J. Phys.* **6** 7–17

Kharadly M M Z and Ross R 2001 Effect of wet antenna attenuation on propagation data statistics *IEEE Trans. Antennas Propag.* **49** 1183–91

Kidd C A, Becker A, Huffman G J, Muller C L, Joe P, Skofronick-Jackson G and Kirschbaum D B 2017 So, how much of the Earth's surface is covered by rain gauges? *Bull. Am. Meteorol. Soc.* **98** 69–78

Kidd C and Huffman G 2011 Global precipitation measurement *Meteorol. Appl.* **18** 334–53

Leijnse H, Uijlenhoet R and Stricker J N M 2007a Rainfall measurement using radio links from cellular communication networks *Water Resour. Res.* **43** W03201

Leijnse H, Uijlenhoet R and Stricker J N M 2007b Hydrometeorological application of a microwave link: 2. Precipitation *Water Resour. Res.* **43** W04417

Leijnse H, Uijlenhoet R and Stricker J N M 2008 Microwave link rainfall estimation: effects of link length and frequency, temporal sampling, power resolution and wet antenna attenuation *Adv. Water Resour.* **31** 1481–93

Li Z *et al* 2021 Two-decades of GPM IMERG early and final run products intercomparison: similarity and difference in climatology, rates and extremes *J. Hydrol.* **594** 125975

Liu Z, Ostrenga D, Teng W and Kempler S 2012 Tropical rainfall measuring mission (TRMM) precipitation data and services for research and applications *Bull. Am. Meteorol. Soc.* **93** 1317–25

Lorenz C and Kunstmann H 2012 The hydrological cycle in three state-of-the-art reanalyses: intercomparison and performance analysis *J. Hydrometeorol.* **13** 1397–420

Malmgren B A, Hulugalla R, Hayashi Y and Mikami T 2003 Precipitation trends in Sri Lanka since the 1870s and relationships to El Niño–southern oscillation *Int. J. Climatol.* **23** 1235–52

MEMO 2020 MEMO | SMHI: microwave-based environmental monitoring (available at: https://smhi.se/memo) (Accessed 30 December 2020)

Mercier F, Barthès L and Mallet C 2015 Estimation of finescale rainfall fields using broadcast TV satellite links and a 4DVAR assimilation method *J. Atmos. Ocean Technol.* **32** 1709–28

Messer H A, Zinevich A and Alpert P 2006 Environmental monitoring by wireless communication networks *Science* **312** 713

Messer H and Sendik O 2015 A new approach to precipitation monitoring *IEEE Signal Process. Mag.* **32** 110–22

Muller C L, Chapman L, Johnston S, Kidd C, Illingworth S, Foody G, Overeem A and Leigh R R 2015 Crowdsourcing for climate and atmospheric sciences: current status and future potential *Int. J. Climatol.* **35** 3185–203

NASA 2021a TRMM (available at: https://trmm.gsfc.nasa.gov/) (Accessed 10 June 2021)

NASA 2021b Two decades of precipitation measurement | NASA global precipitation measurement (available at: www.gpm.nasa.gov/missions/two-decades-precipitation-measurement) (Accessed 10 June 2021)

Nisansala W D S, Abeysingha N S, Islam A and Bandara A M K R 2020 Recent rainfall trend over Sri Lanka (1987–2017) *Int. J. Climatol.* **40** 3417–35

Olsen R L, Rogers D V and Hodge D B 1978 The $aR^b$ relation in the calculation of rain attenuation *IEEE Trans. Antennas Propag.* **26** 318–29

Olson W S and the GPM Combined Radar-Radiometer Algorithm Team 2018 GPM combined radar-radiometer precipitation algorithm theoretical basis document (Version 5) (available at: https://gpm.nasa.gov/sites/default/files/2020-05/Combined_algorithm_ATBD.V05.pdf) (Accessed 30 December 2020)

Overeem A 2021 Gridded rainfall maps retrieved from commercial microwave link (CML) data from Sri Lanka *4TU.ResearchData. Dataset* (https://doi.org/10.4121/14166539.v2)

Overeem A, Leijnse H and Uijlenhoet R 2011 Measuring urban rainfall using microwave links from commercial cellular communication networks *Water Resour. Res.* **47** W12505

Overeem A, Leijnse H and Uijlenhoet R 2013 Country-wide rainfall maps from cellular communication networks *Proc. Natl Acad. Sci. USA* **110** 2741–5

Overeem A, Leijnse H and Uijlenhoet R 2016a Retrieval algorithm for rainfall mapping from microwave links in a cellular communication network *Atmos. Meas. Tech.* **9** 2425–44

Overeem A, Leijnse H and Uijlenhoet R 2016b Two and a half years of country-wide rainfall maps using radio links from commercial cellular telecommunication networks *Water Resour. Res.* **52** 8039–65

Overeem A, Leijnse H and Uijlenhoet R 2012 Quantitative precipitation estimation using commercial microwave links *Proc. Symp. on Weather Radar and Hydrology (Exeter, UK, April 2011)* vol 351 ed R J Moore, S J Cole and A J Illingworth (Wallingford: IAHS Press) pp 129–34

Pollock M D *et al* 2018 Quantifying and mitigating wind-induced undercatch in rainfall measurements *Water Resour. Res.* **54** 3863–75

Polz J, Chwala C, Graf M and Kunstmann H 2020 Rain event detection in commercial microwave link attenuation data using convolutional neural networks *Atmos. Meas. Tech.* **13** 3835–53

Rabiei E, Haberlandt U, Sester M and Fitzner D 2013 Rainfall estimation using moving cars as rain gauges—laboratory experiments *Hydrol. Earth Syst. Sci.* **17** 4701–12

RAINLINK 2020 Github—overeem11/RAINLINK: retrieval algorithm for rainfall mapping from microwave links in a cellular communication network (available at: https://github.com/overeem11/RAINLINK) (Accessed 30 December 2020)

Rayitsfeld A, Samuels R, Zinevich A, Hadar U and Alpert P 2012 Comparison of two methodologies for long term rainfall monitoring using a commercial microwave communication system *Atmos. Res.* **104–105** 119–27

Rios Gaona M F, Overeem A, Brasjen A M, Meirink J F, Leijnse H and Uijlenhoet R 2017 Evaluation of rainfall products derived from satellites and microwave links for the Netherlands *IEEE Trans. Geosci. Remote Sens.* **55** 6849–59

Rios Gaona M F, Overeem A, Raupach T H, Leijnse H and Uijlenhoet R 2018 Rainfall retrieval with commercial microwave links in São Paulo, Brazil *Atmos. Meas. Tech.* **11** 4465–76

Roversi G, Alberoni P P, Fornasiero A and Porcù F 2020 Commercial microwave links as a tool for operational rainfall monitoring in Northern Italy *Atmos. Meas. Tech.* **13** 5779–97

Saltikoff E *et al* 2019 An overview of using weather radar for climatological studies: successes, challenges and potential *Bull. Am. Meteorol. Soc.* **100** 1739–52

Schleiss M, Rieckermann J and Berne A 2013 Quantification and modeling of wet-antenna attenuation for commercial microwave links *IEEE Geosci. Remote Sens.* **10** 1195–9

Skofronick-Jackson G *et al* 2017 The global precipitation measurement (GPM) mission for science and society *Bull. Am. Meteorol. Soc.* **98** 1679–95

Skofronick-Jackson G, Kirschbaum D, Petersen W, Huffman G, Kidd C, Stocker E and Kakar R 2018 The global precipitation measurement (GPM) mission's scientific achievements and societal contributions: reviewing four years of advanced rain and snow observations *Q. J. R. Meteorol. Soc.* **144** 27–48

Sohail Afzal M, Shah S H H, Cheema M J M and Ahmad R 2018 Real time rainfall estimation using microwave signals of cellular communication networks: a case study of Faisalabad, Pakistan *Hydrol. Earth Syst. Sci. Discuss.* (https://doi.org/10.5194/hess-2017-740)

Sri Lanka Department of Meteorology 2020 Climate of Sri Lanka (available at: www.meteo.gov.lk/index.php?option=com_content&view=article&id=94&Itemid=310&lang=en&lang=en#2-southwest-monsoon-season-may-september) (Accessed 30 December 2020)

Steiner M, Smith J A, Burges S J, Alonso C V and Darden R W 1999 Effect of bias adjustment and rain gauge data quality control on radar rainfall estimation *Water Resour. Res.* **35** 2487–503

Uijlenhoet R, Overeem A and Leijnse H 2018 Opportunistic remote sensing of rainfall using microwave links from cellular communication networks *WIREs Water* **5** e1289

Upton G J G, Holt A R, Cummings R J, Rahimi A R and Goddard J W F 2005 Microwave links: the future for urban rainfall measurement? *Atmos. Res.* **77** 300–12

Van Leth T C, Overeem A, Leijnse H and Uijlenhoet R 2018 A measurement campaign to assess sources of error in microwave link rainfall estimation *Atmos. Meas. Tech.* **11** 4645–69

Wang Z, Schleiss M, Jaffrain J, Berne A and Rieckermann J 2012 Using Markov switching models to infer dry and rainy periods from telecommunication microwave link signals *Atmos. Meas. Tech.* **5** 1847–59

Wolff W, Overeem A, Leijnse H and Uijlenhoet R 2021 Rainfall retrieval algorithm for commercial microwave links: stochastic calibration *Atmos. Meas. Tech. Discuss.* (https://doi.org/10.5194/amt-2021-34)

Zheng F *et al* 2018 Crowdsourcing methods for data collection in geophysics: state of the art, issues and future directions *Rev. Geophys.* **56** 698–740